

---

# Challenges in Modeling the X-29A Flight Test Performance

---

John W. Hicks

Ames Research Center, Dryden Flight Research Facility, Edwards, California

Jan Kania

Air Force Flight Test Center, Edwards Air Force Base, California

Robert Pearce and Glen Mills

Grumman Aerospace Corp., Edwards, California

1987



National Aeronautics and  
Space Administration

**Ames Research Center**

Dryden Flight Research Facility  
Edwards, California 93523-5000



# CHALLENGES IN MODELING THE X-29A FLIGHT TEST PERFORMANCE

John W. Hicks\*  
NASA Ames Research Center  
Dryden Flight Research Facility  
Edwards, California

Jan Kania\*\*  
6520th Test Group/ENF  
Air Force Flight Test Center  
Edwards Air Force Base, California

and

Robert Pearce† and Glen Mills‡  
Grumman Aerospace Corp.  
Edwards, California

## Abstract

The paper presents the methods, instrumentation, and difficulties associated with drag measurement of the X-29A aircraft. The initial performance objective of the X-29A program emphasized drag polar shapes rather than absolute drag levels. Priorities during the flight envelope expansion restricted the evaluation of aircraft performance. Changes in aircraft configuration, uncertainties in angle-of-attack calibration, and limitations in instrumentation complicated the analysis. Limited engine instrumentation with uncertainties in overall in-flight thrust accuracy made it difficult to obtain reliable values of coefficient of parasite drag. The aircraft was incapable of tracking the automatic camber control trim schedule for optimum wing flaperon deflection during typical dynamic performance maneuvers; this has also complicated the drag polar shape modeling. The X-29A was far enough off the schedule that the developed trim drag correction procedure has proven inadequate. Despite these obstacles, good drag polar shapes have been developed throughout the flight envelope. Preliminary flight results have compared well with wind tunnel predictions. A more comprehensive analysis must be done to complete the performance models. The detailed flight performance program with a calibrated engine will benefit from the experience gained during this preliminary performance phase.

## Nomenclature

ACC	automatic camber control
$C_D$	coefficient of total drag
$C_{D_i}$	coefficient of induced drag
$C_{D_{min}}$	coefficient of parasite drag
$C_L$	coefficient of lift
cg	center of gravity
D	aircraft drag
$F_{ex}$	excess thrust
$F_G$	gross thrust

$F_N$	net thrust available
FCS	flight control system
FDMS	flight deflection measurement system
FSW	forward-swept wing
g	normal load factor
L	aircraft lift
LED	light-emitting diode
MCC	manual camber control
$n_z$	wind-axis normal load factor
q	dynamic pressure
S	reference wing area
W	gross weight of aircraft
$\alpha$	angle of attack
$\beta$	angle of sideslip
$\Delta C_D$	incremental change in coefficient of drag
$\delta_c$	canard deflection
$\delta_f$	flaperon deflection
$\delta_s$	strake flap deflection

## Introduction

Aircraft performance modeling to obtain detailed thrust-drag models has been evolving for a number of years. The objectives of dynamic flight techniques, precise thrust-drag accounting, advanced modeling techniques, and new in-flight instrumentation have been to develop the most accurate aerodynamic drag model of the airframe. External factors such as highly augmented flight control systems, complex inlet-engine combinations, and aeroelastic effects have complicated the modeling task. Examples of an extensive effort in detailed thrust-drag modeling were the studies undertaken on the transonic aircraft technology F-111A project<sup>1</sup> and the XB-70 program.<sup>2-5</sup> The advanced technology demonstrator X-29A research aircraft has provided data for the performance modeling of a highly unstable, highly augmented, three-control-surface air-

\*Chief Engineer, X-29 Program, AIAA Member.

\*\*Performance Engineer, X-29 Program.

†Aerodynamics Engineer, X-29 Program.

‡Performance Engineer, X-29 Program, AIAA Member.

craft with a forward-swept-wing/canard aerodynamic configuration.

The X-29A project was initiated by the Defense Advanced Research Projects Agency in 1977. The aircraft was designed and built by Grumman Aerospace Corp. In October 1984, it was shipped to the Dryden Flight Research Facility of NASA Ames Research Center (Ames-Dryden), with its first test flight conducted on December 14, 1984. The flight test team consisted of personnel from Ames-Dryden, the U.S. Air Force Flight Test Center, and the Grumman Corp.; Ames-Dryden was the responsible test organization.

The primary objective of this phase of the X-29A program was to expand the 1-g and maneuver flight envelopes. This took priority over other flight research objectives such as performance and flying qualities.<sup>6</sup> The performance maneuvers during this test phase were limited. The emphasis was to obtain accurate induced drag polar shapes over the Mach number range rather than to obtain absolute drag levels. This paper describes the challenges encountered in determining the preliminary drag polar model for the X-29A aircraft. It includes a discussion of the test techniques, the aircraft instrumentation system, the limitations in obtaining flight data, and the difficulties encountered in the analysis.

#### Aircraft Description

The X-29A aircraft (Fig. 1) is a single-seat, fighter-type aircraft with a forward-swept wing (FSW). It has a highly relaxed static stability that is nominally set at a 35-percent negative static margin. The FSW has upper- and lower-wing skins of graphite-epoxy composite. Aeroelastic tailoring is used to control wing deflection and to inhibit wing structural divergence. The thin supercritical airfoil has a cross section of 5 percent mean chord thickness with no leading-edge devices; it incorporates trailing-edge flaperons with a manual camber control (MCC) flight control mode and an automatic camber control (ACC) mode. The double-hinged flaperons are in three sections on each wing with midwing and outboard flaperons driven by a single actuator. They provide high lift during takeoff and landing and provide variable camber to increase aerodynamic efficiency over the entire flight envelope. The 33.73° quarter-chord forward sweep of the wings is complemented by close-coupled canards and aft-mounted strake flaps. The canards, flaperons, and strake flaps work together for trim and pitch control. Full-span differential flaperons provide roll control, and a single-piece rudder gives yaw control. Canards deflect from 30° leading edge up to 60° leading edge down. Flaperons travel from -10° trailing edge up to 24.75° trailing edge down. Strake flaps have a full  $\pm 30^\circ$  of travel. A digital-analog triplex fly-by-wire flight control system (FCS) has a 40-Hz update rate in each flight axis to artificially stabilize the large negative static margin of the aircraft.

The MCC wing mode allows the pilot to set fixed, discrete flaperon positions in 5° increments from -5° trailing edge up to 24.75° trailing edge down. The flaperons remain fixed in this

mode until the canard stall-protection logic forces the flaperons to move. Presently, MCC is used for fixing the wing configuration for structural wing divergence clearance; little performance work in the MCC flaperon mode has been done to date.

The aircraft is powered by a single General Electric F404-GE-400 afterburning turbofan engine that is in the 16,000-lb-thrust class. The side-mounted engine inlets are a simple, fixed configuration that optimizes flight in the transonic region. Four internally mounted fuel tanks have a total capacity of 4000 lb, which results in an aircraft takeoff gross weight  $W$  of 17,800 lb.

The X-29A research aircraft integrates several multidisciplinary technologies in a synergistic manner for conducting flight research of the individual technologies and for validating the technological data base used to develop the aircraft. The technologies as related to the predicted increased performance capabilities of the X-29A aircraft include the FSW and the close-coupled canard for a wing-canard elliptical lift span-loading. The FSW has less leading-edge sweep than an aft-swept wing with an equivalent shock sweep angle. The incorporated thin supercritical airfoil has experimentally demonstrated less profile drag for decreasing leading-edge sweep. Thus, the FSW will have less profile drag than the equivalent aft-swept wing and will be able to sustain higher lift coefficients.

The wing-canard combination provides mutually beneficial aerodynamic interaction; that is, the wing upwashes the canard to provide increased effective angle of attack  $\alpha$  for the canard, and the canard downwashes the wing to delay root stall. The wing root is characteristically where stall begins on an FSW aircraft. The wing incorporates a discrete variable-camber system that, together with relaxed static stability and the ACC mode, provides optimum aerodynamic efficiency with minimum trim drag throughout the flight envelope. A more detailed discussion of the specific advanced aerodynamic technologies can be found in Ref. 7.

#### Wind Tunnel Data Base

Grumman Aerospace Corp. conducted three wind tunnel tests during the development of the X-29A aircraft. These included tests conducted in May 1982 at the NASA Ames Research Center 11-Foot Transonic Wind Tunnel and the 9- by 7-Foot Supersonic Wind Tunnel facilities<sup>8</sup> and tests conducted in March 1983 at the Grumman 7- by 10-Foot Low-Speed Tunnel using a rigid 1/8th-scale model. A supplemental test was carried out in July 1983 by Ames-Dryden at the NASA Ames 11-Foot Tunnel.<sup>9</sup>

The primary objectives of these tunnel tests were to obtain structural loads data and aerodynamic derivative data, and not to measure minimum coefficient of drag  $C_{D_{min}}$ . The wind tunnel data were incorporated into a full nonlinear aerodynamic data base that has been adjusted for structural flexibility.<sup>10</sup> These data provided the basis for the aerodynamic and flight controls

analysis and are incorporated into the X-29A simulator. The wind tunnel data were also used to develop the ACC schedule for maximum aerodynamic efficiency and to obtain a detailed measurement of drag buildup in the individual airframe components.<sup>11</sup>

#### Flight Test Instrumentation

The X-29A onboard instrumentation system consists of constant-bandwidth frequency modulation and a 10-bit pulse-code modulation system. The pulse-code modulation system has five separate modules that are combined in an interleaver unit with FCS information from an AirResearch 429 data bus. The aircraft is instrumented for structural loads and dynamics, flight controls, stability and control, aircraft subsystems, and performance. Parameters are measured at various sampling rates from 25 to 400 samples/sec. All data are telemetered to the ground for real-time monitoring and data analysis and represent the sole source of data acquisition. Control room displays include the usual eight-channel strip charts and cathode-ray-tube displays of digital and time history analog data as well as computed results.

The left wing, canard, and strake flap are instrumented with a total of 179 flush-mounted pressure measurement points in 5 rows on the wing, 2 rows on the canard, and 1 row down the strake and strake flap. Twelve infrared light-emitting diode (LED) sensors that form part of the flight deflection measurement system (FDMS) are mounted on the upper surface of the right wing. The sensor receiver is mounted in the fuselage side at the wing root (Fig. 2). Each wing has a flaperon structural excitation shaker system with an eccentric rotary mass (Fig. 3) mounted at the base of the outboard flaperon actuator housing. The shaker excitation system and the FDMS were temporary external flight test instrumentation and were not part of the basic aircraft. They did, however, have some aerodynamic effect on the aircraft.

The performance instrumentation package consists mainly of two separate body-mounted three-axis accelerometer systems. One is referred to as the center-of-gravity (cg) accelerometer package; it has larger range accelerometers than the second system. Its longitudinal accelerometer range is  $\pm 1$  g, its normal accelerometer range is from -3 g to 8 g, and its lateral accelerometer range is  $\pm 1$  g. The second system referred to as the dynamic performance cg package has smaller accelerometer ranges specifically sized for dynamic performance pushover-pullup maneuvers. Its longitudinal accelerometer range is  $\pm 0.6$  g, its normal accelerometer range is -1 g to 3 g, and its lateral accelerometer range is  $\pm 0.6$  g. In addition, a three-axis rate gyro package measures pitch, roll, and yaw attitudes and rates, as well as angular accelerations. The sampling rate for these parameters is 120 samples/sec. A Grumman F-14 flight-test nose boom (Fig. 4) was used to obtain pitot static measurements. Vanes on the nose boom provided measurements of  $\alpha$  and angle of sideslip  $\beta$ .

The F404-GE-400 engine has the General Electric basic kit instrumentation that measures inlet temperature, compressor and turbine speeds

and pressures, combustor pressure, and turbine exhaust temperature. This instrumentation makes use of a single production exhaust pressure measurement on the turbine and a main-engine fuel mass flowmeter. The basic kit instrumentation was primarily intended to monitor engine operating levels and engine health, but not to accurately measure in-flight gross thrust  $F_g$ . The kit lacks the volumetric main engine and afterburner fuel flow measurements and the 20-probe turbine exhaust pressure rake used in the full flight-test thrust kit. The installed engine had all the full F-18 flight-test thrust components. However, it was decided early in the X-29A program that the additional components of the full thrust kit would not be connected because the primary project objective in drag measurement was to obtain drag polar shapes only. Sensitivity analysis by the engine manufacturer has shown that the uninstalled thrust uncertainty level of the basic kit is nominally  $\pm 5.0$  percent and could be as high as  $\pm 7.9$  percent, depending on the flight condition. The in-flight thrust calculation is presently unable to calculate in-flight  $F_g$  in afterburner operation due to a lack of afterburner fuel flow. Two of the project F404 engines, serial numbers 215209 and 215213, have full thrust kits in place; one engine, serial number 215215, has only the basic kit. Table 1 summarizes the engine configurations and their use.

Because of the subsequent requirement for more accurate measurement of in-flight  $F_g$ , and thus drag  $D$ , and to assist in careful thrust-drag accounting, X-29A engine serial number 215209 was calibrated at the Propulsion System Laboratory of NASA Lewis Research Center from late 1985 to early 1986. This was done using the full thrust kit and selecting a test point matrix that covered the entire X-29A flight envelope. About 160 test points were measured from flight idle power to maximum afterburning thrust. The resulting data base was used to correct the generic in-flight thrust computer program. In addition, pressures in the nozzle afterburner were obtained at static pressure orifices, and the data were used to develop a simplified gross thrust method for real-time analysis.<sup>12</sup>

After the calibrated engine has been installed and the thrust computer program corrected, the corrected in-flight thrust computation accuracy is predicted to be within  $\pm 1.5$  percent. The real-time simplified  $F_g$  calculation is predicted to be within  $\pm 1.8$  percent. Reference 13 contains a sensitivity analysis of the effect of various engine parameter measurement errors on in-flight thrust accuracy for the F404 engine.

#### Flight Test Approach

The performance drag modeling maneuvers consisted of dynamic maneuver techniques to obtain a continuous  $\alpha$  range. A 30-sec stabilized point preceded the dynamic maneuvers. This was followed by a 20-sec pushover-pullup maneuver from 1-g stabilized flight to a pushover to 0 g and a pullup to 2 g and then back to stabilized 1-g flight at the power-for-level-flight condition. This covered the lower to medium levels of coefficient of lift  $C_L$ . A windup turn at constant thrust and

Mach number was then flown from stabilized flight to the specified load factor  $n_z$  and/or the  $\alpha$  limit by exchanging altitude for airspeed to maintain constant Mach number. The middle to high  $C_L$  range was developed with the windup turn.

The structural load limit was set at 6.4 g, which was 80 percent of the design load limit and was based on the fact that X-29A was only proof-loaded to the design load limit. Performance maneuvers flown during the envelope expansion process were limited initially to  $\alpha = 15^\circ$  and to the load factors cleared at the time of flight. The maneuvers were also limited in buffet intensity levels at the wingtip and were not to exceed  $\pm 4$  g above the nominal load factor. All maneuvers were flown from 10,000 to 40,000 ft.

#### Data Analysis

Aircraft  $C_D$  and  $C_L$  were calculated from the equations

$$C_D = \frac{D}{qS} = \frac{F_N - F_{ex}}{qS}$$

$$C_L = \frac{L}{qS} = \frac{n_z W - F_G \sin \alpha}{qS}$$

where

$F_{ex}$  = excess thrust

$F_N$  = net thrust available

$L$  = aircraft lift

$q$  = dynamic pressure

$S$  = reference wing area

The in-flight thrust calculation procedure is extensive and can be found in Reference 14. Reference 15 reports on a drag polar sensitivity study that analyzed the error sources and their relative magnitude in the  $C_D$  and  $C_L$  calculations.

The purpose of the drag correction procedure in the performance analysis program was to adjust the flight test data to the power-off, trimmed ACC schedule configuration as used in the generation of the wind tunnel data base. The method was only capable of providing trim drag correction of the data for  $\alpha < \pm 2^\circ$  from the ACC trim schedule. Similarly, the control surface schedules could only be adjusted for control surface deflection up to  $\pm 5^\circ$  from the ACC trim schedule. Depending on flight conditions, this corresponded to drag adjustments up to  $C_L = 1.0$ .

Other drag corrections incorporated in the analysis program included body-axis accelerometer angular rate and acceleration adjustments. Thrust corrections included estimated nozzle and spillage drag, as well as calculated ram drag corrections. A thrust moment contribution to the drag polar was also taken into account. Trim drag adjustments for off-reference cg were also made.

The trim drag correction program could not be used on some flight data where the aircraft control surface configuration was substantially off the ACC schedule. A comparison program was used to correlate the flight-test dynamic polar and lift curves with the equivalent wind tunnel data predictions. The program used the flight time history of flight conditions, cg,  $\alpha$ , and control surface positions to query the aerodynamic data base for the polar and lift curve data. In this way, untrimmed flight results could be compared to the wind tunnel data.

#### Aircraft Test Configuration

The X-29A external airframe configuration has not remained fixed during the envelope expansion phase of the program. To aid the in-flight monitoring of wing deflections, beginning with flight 9, the FDMS was added to the surface of the upper right wing. The twelve FDMS targets ranged in size from 0.25 to 1.50 in high. The protuberance drag contribution and the added skin friction drag from localized turbulence from the FDMS targets were difficult to measure; their effect on the overall airframe drag is unknown.

Figure 5 shows the effect of the FDMS drag increment on the drag polar model. For flow visualization, flow cones and tufts were placed on the upper surface of the left wing during flights 12, 13, and 16. After flight 19, the flaperon shaker excitation system was added to each wing at the aft end of the outboard flaperon actuator housing. A modified actuator fairing was required to enclose the shaker (Fig. 6). This probably changed the base drag behind the wings.

Attempts to isolate the drag increments  $C_D$  of these configurations changes have been difficult because of uncertain  $C_{D_{min}}$  measurements. Maneuver dynamics resulting in slightly different control surface scheduling also added to the complexity of determining  $C_D$ . Figure 7 shows the drag changes with and without the flaperon shaker system installed.

An FCS software modification after flight 23 effectively changed the aircraft configuration at certain flight conditions. The software change corrected an anomaly in the ACC flaperon saturation logic that was discovered early in the flight program. The proper operation of the ACC logic is to integrate the strake flap position to keep the canards on their trim schedule as the flaperons become saturated in the fully down position. The anomaly occurred when the aileron inputs by the pilot prevented the FCS computers from recognizing the fully down flaperons as saturated. This consequently did not allow the strake flaps to follow the integration logic. The software change corrected the problem by allowing the computers to recognize the fully down flaperons as saturated even with aileron input. However, this changed the overall trimmed ACC schedule tracking of the canard and strake flaps during maneuvering and resulted in different trim drag levels. Figure 8 shows the reduced drag improvements at higher  $C_L$  with the modified FCS software. Table 2 summa-

izes the configuration changes of the X-29A during the envelope expansion phase.

### Results and Discussion

Several factors affected the aerodynamic performance of the X-29A aircraft and the analysis during the envelope expansion phase: (1) the addition of flight test instrumentation that influenced external aerodynamics, (2) the FCS modifications that changed control surface positions, (3) the off-ACC mode schedule as a function of maneuver dynamics, (4) the difficulties in obtaining an accurate  $\alpha$  calibration, and (5) uncertainties of the thrust accuracy. The last two factors led to uncertainties in  $C_{Dmin}$  values.

The  $\alpha$  calibration was particularly difficult on the X-29A aircraft. Calibration results from the pitch-attitude method were not consistent because the aircraft was difficult to stabilize at a given airspeed and altitude. The X-29A aircraft attempts to stabilize at a zero pitch rate. Even with 40-Hz anti-aliasing filters,  $\alpha$  and  $\beta$  measurements from the nose-boom system were very noisy, due to aeroservoelastic interaction with the modal characteristics of the nose boom. This contributed to data scatter and an unexplained  $1^\circ$  bias in the  $\alpha$  calibration results. In addition, both  $\alpha$  and  $\beta$  measurements suffered from small ( $\pm 0.5^\circ$ ) random step changes on occasion during stabilized flight. These step changes are believed to be due to local flow angularities on the nose boom, which impact the boom vanes. The effect of uncertainty on the drag polar shape due to  $\alpha$  calibration variations (Fig. 9) has a significant influence on drag polar modeling. This error is introduced through the  $\alpha$  and  $\beta$  transformation of body-axis accelerations to wind-axis accelerations and in the changing of thrust components to lift. Efforts to obtain an accurate calibration are continuing.

The FCS was designed for overall aircraft stabilization of an unstable airframe and only washes out to the ACC schedule as the aircraft stabilizes at a given pitch rate. The ACC mode, which is intended to hold the optimum L/D ratio during trimmed flight, was not successful in staying on schedule in highly dynamic maneuvers. As indicated in Fig. 10, the flaperons were as much as  $12^\circ$  off the ACC schedule as a function of maneuver rate during windup turns. The canards were as much as  $10^\circ$  off the ACC schedule, and the strake flaps as much as  $7^\circ$  off. Being off the optimal aerodynamic configuration resulted in an added drag penalty for the airframe. The  $\Delta C_D$  between the untrimmed dynamic polar model and the drag polar model predicted from the trimmed ACC schedule was as much as 250 drag counts. Windup turn maneuver rates were varied from 5 to 20 sec, which did not seem to affect the measured drag levels in the low subsonic Mach regime. However, the maneuver rate did show an effect on dynamic drag levels at transonic Mach numbers. The dynamics levels of the maneuvers have not been fully adjusted to the trimmed polar model in the data reduction computer programs.

Grumman Aerospace Corp. suggested a method for improving the flaperon tracking of the ACC sched-

ule by increasing the gain on the FCS canard error signal that drives the flaperon rate. Increasing the gain increases the flaperon ACC tracking rate during the dynamic maneuvers. The present gain of 0.4 would therefore be increased to 1.6. This would bring the aircraft control surfaces very close to the trimmed ACC schedule, with only a small degradation in the FCS stability margins. (The FCS has minimum margins of 3 dB in gain and  $22.5^\circ$  in phase.) Predictions show that this increased gain in the canard error signal can improve performance by more closely tracking the optimum ACC schedule during maneuvering. It also allows the drag correction procedure to adjust for the remaining off-schedule positions of the control surfaces. The plan is to implement this method during the X-29A follow-on flight research phase in 1987.

As shown in Fig. 11, the net scatter in the drag polar data is about  $\pm 50$  drag counts at a given Mach value. A calibrated engine is expected to improve the overall polar results; however, this data scatter is considered sufficient flight test results to determine the drag polar shapes. The present plan is to install the calibrated F404 engine in the aircraft in late 1986 for the detailed follow-on flight research phase in 1987.

Typical drag polar results are shown in Fig. 12. The preliminary dynamic untrimmed flight results show the X-29A performance is at least as good as predicted. The consistency of the measured polar shapes are particularly good. The  $C_{Dmin}$  values are not considered reliable until the calibrated engine is installed. This engine will also allow for a more accurate thrust-drag accounting and will possibly improve the understanding of the polar shapes and the individual  $\Delta C_D$  increments more precisely.

### Concluding Remarks

The performance drag polar modeling of the X-29A advanced technology aircraft during the initial flight envelope expansion phase has presented numerous challenges. External airframe configuration changes have added uncertainties to the flight test results. Uncertainties in the angle-of-attack calibration have affected the polar results and have been difficult to analyze. Maneuver dynamics have affected the tracking of the automatic camber control trim schedule for optimum wing flaperon deflection. This in turn affected the untrimmed data, which have larger control-surface deviations than the analysis programs can successfully correct.

The challenges of the thrust-drag accounting and analysis have nevertheless yielded reliable results, particularly in determining the induced drag polar shapes. The preliminary polar shapes have met or slightly exceeded predictions for the Mach number range tested. Due to the questionable in-flight thrust calculation accuracy of the basic kit of the General Electric F404-GE-400 engine, the measured minimum parasite drag levels of the X-29A aircraft have not been considered accurate. Better accuracy will be provided when the calibrated engine, serial number 215209, is installed in the aircraft. In addition, future plans for

the follow-on flight research phase include the installation of an improved nose-boom system for better measurements of angle of attack and sideslip, airspeed, and altitude. Experience gained from this preliminary performance phase of the X-29A aircraft should benefit the follow-on performance research phase.

#### References

<sup>1</sup>Cooper, J.M., Jr., Hughes, D.L., and Rawlings, K., III, "Transonic Aircraft Technology: Flight-Derived Lift and Drag Characteristics," Report AD-B024380L, AFFTC-TR-77-12, Vol. 1, 1977.

<sup>2</sup>Arnaiz, H.H., "Flight-Measured Lift and Drag Characteristics of a Large, Flexible, High Supersonic Cruise Airplane," NASA TM-X-3532, 1977.

<sup>3</sup>Daugherty, J.C., "Wind-Tunnel/Flight Correlation Study of Aerodynamic Characteristics of a Large Flexible Supersonic Cruise Airplane (XB-70-1): Part I - Wind-Tunnel Tests of a 0.03-Scale Model at Mach Numbers From 0.6 to 2.53," NASA TP-1514, 1979.

<sup>4</sup>Peterson, J.B., Jr., Mann, M.J., Sorrells, R.B., III, Sawyer, W.C., and Fuller, D.E., "Wind-Tunnel/Flight Correlation Study of Aerodynamic Characteristics of a Large Flexible Supersonic Cruise Airplane (XB-70-1): Part II - Extrapolation of Wind-Tunnel Data to Full-Scale Conditions," NASA TP-1515, 1980.

<sup>5</sup>Arnaiz, H.H., Peterson, J.B., Jr., and Daugherty, J.C., "Wind-Tunnel/Flight Correlation Study of Aerodynamic Characteristics of a Large Flexible Supersonic Cruise Airplane (XB-70-1): Part III - A Comparison Between Characteristics Predicted From Wind-Tunnel Measurements and Those Measured in Flight," NASA TP-1516, 1980.

<sup>6</sup>Sefic, W.J. and Cutler, W., "X-29A Advanced Technology Demonstrator Program Overview," AIAA Paper 86-9727, April 1986.

<sup>7</sup>Moore, M. and Frei, D., "X-29 Forward Swept Wing Aerodynamic Overview," AIAA Paper 83-1834, July 1983.

<sup>8</sup>Charletta, R., "Series I Transonic/Supersonic Testing on a 12.5% Scale Grumman Design 712, X-29A Forward-Swept Wing Demonstrator Model in the NASA-ARC 11 Foot and 9x7 Foot Wind Tunnels at Moffett, Ca.," AER/T-Ames-538-1-11, 97, Vol. 1 to 3, Grumman Aerospace Corp., 1982.

<sup>9</sup>Bowers, A.H., "X-29A Longitudinal and Directional Force and Moment Supplemental Transonic Wind Tunnel Test Results," NASA TM-85909, 1984.

<sup>10</sup>Frei, D. and Rich, D., "X-29 Flexible, Non-Linear Aerodynamic Math Model; Equations and Computer Subroutines," Grumman Aerospace Corp. Memo 712-Eng-M-83-367, 1983, and "Data Tables - Aero 4," Grumman Aerospace Corp. Memo 712-Eng-M-83-397, Rev. A, 1983.

<sup>11</sup>Frei, D.R., "X-29 - Justification of Estimated Full Scale Trimmed Lift and Flight Polar Based on Aero 4," Grumman Aerospace Corp. Memo 712-Eng-M-84-099, 1984.

<sup>12</sup>Hughes, D.L., "Comparison of Three Thrust Calculation Methods Using In-Flight Thrust Data," NASA TM-81360, 1981.

<sup>13</sup>Hughes, D.L., Ray, R.J., and Walton, J.T., "Net Thrust Calculation Sensitivity of an Afterburning Turbofan Engine to Variations in Input Parameters," AIAA Paper 85-4041, October 1985.

<sup>14</sup>"F404-400 In-Flight Thrust Program No. 83112," General Electric Co., 1983.

<sup>15</sup>Powers, S.G., "Predicted X-29A Lift and Drag Coefficient Uncertainties Caused by Errors in Selected Parameters," NASA TM-86747, 1985.

Table 1 Engine configuration

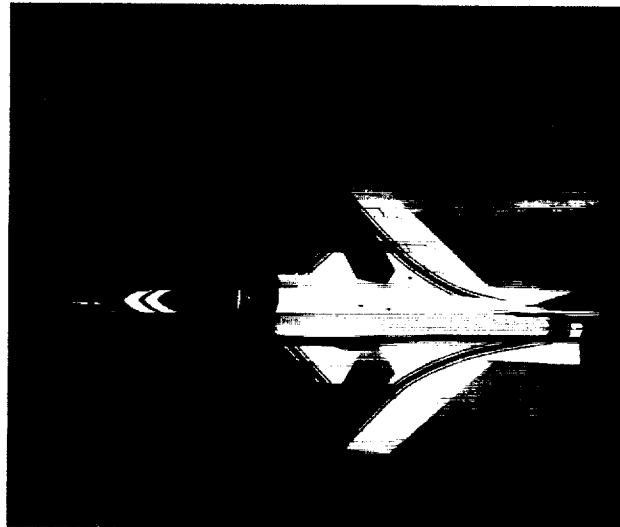
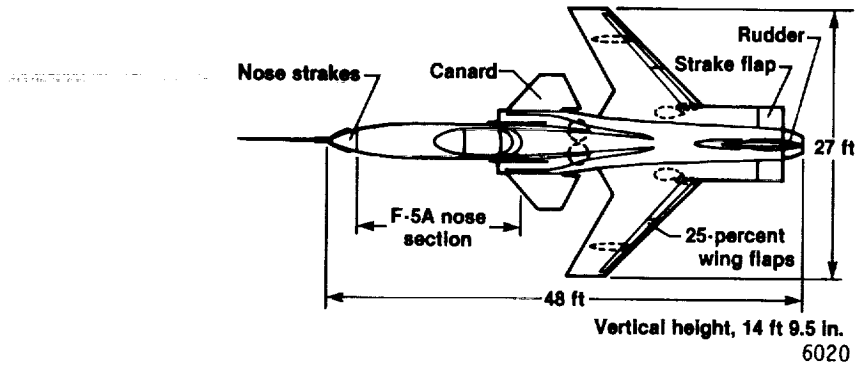
F404 engine	Instrumentation	Use	Calibration
215209	Full thrust kit	Performance flights	Yes
215213	Full thrust kit <sup>a</sup>	Envelope expansion	No
215215	Basic kit	Spare	No

<sup>a</sup>Only basic kit part of full thrust kit activated for flight envelope expansion phase.



Table 2 Aircraft configuration

Flight number	FDMS	Flaperon shaker	Tufts	Original ACC	Modified ACC
1	No	No	No	Yes	No
9	Yes	No	No	Yes	No
12,13,16	Yes	No	Yes	Yes	No
19	Yes	Yes	No	Yes	No
23 to 71	Yes	Yes	No	No	Yes



ECN 33297-009

Fig. 1. Advanced technology demonstrator X-29A aircraft.

ORIGINAL PAGE IS  
OF POOR QUALITY

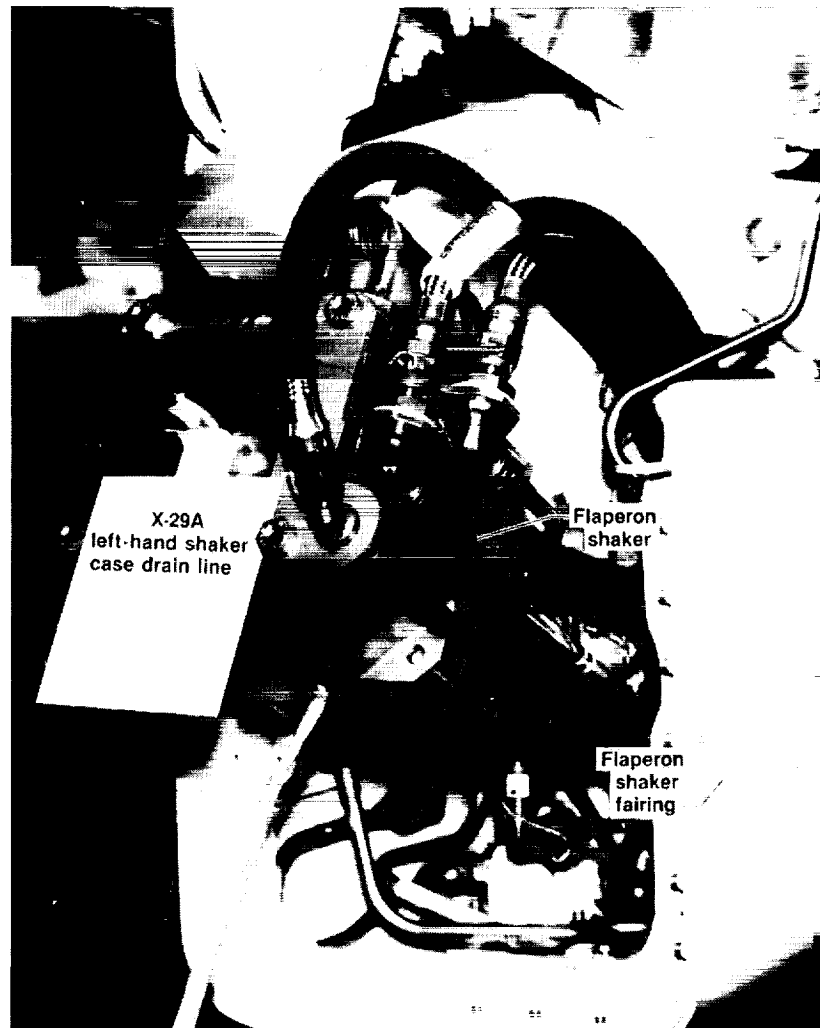
OF POOR QUALITY



6008

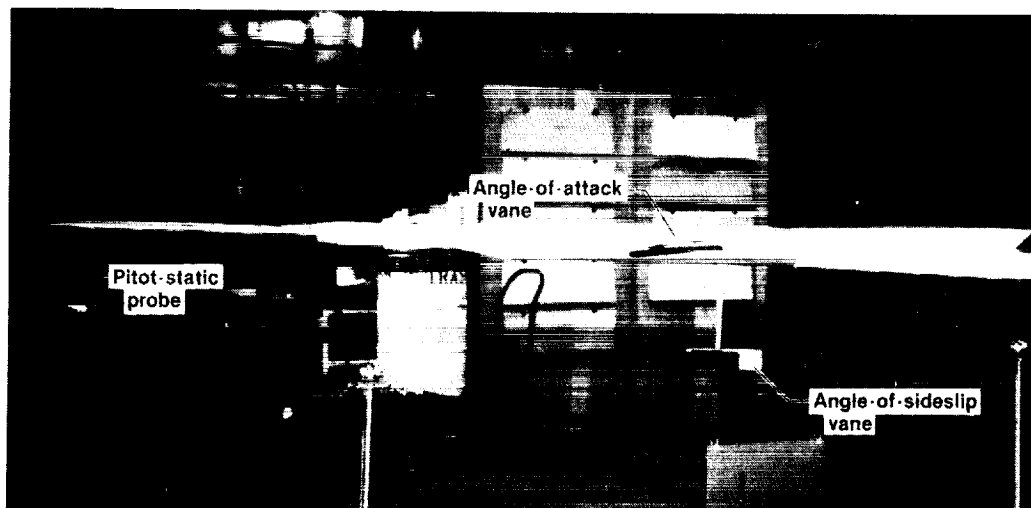
*Fig. 2. Flight deflection measurement system.*

ORIGINAL PAGE IS  
OF POOR QUALITY



6009

*Fig. 3. Flaperon shaker system.*



6010

*Fig. 4. Flight-test nose boom.*

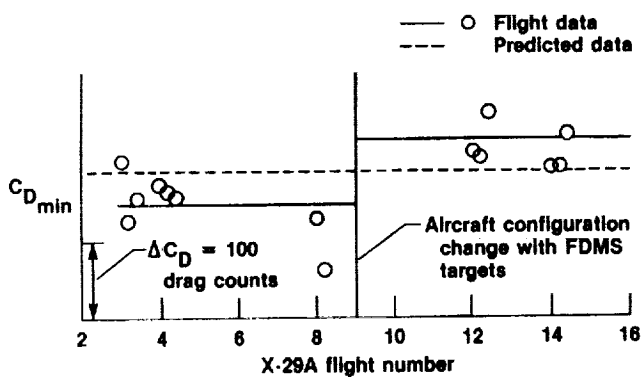
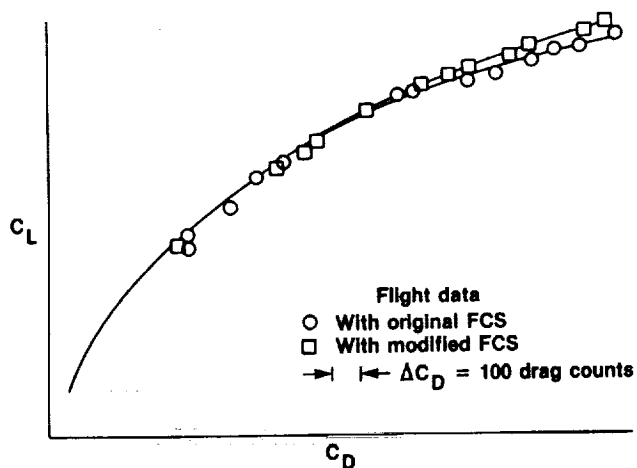


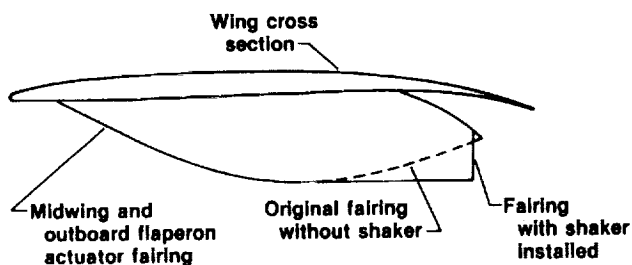
Fig. 5. Effects of FDMS targets on drag polar model.

6011



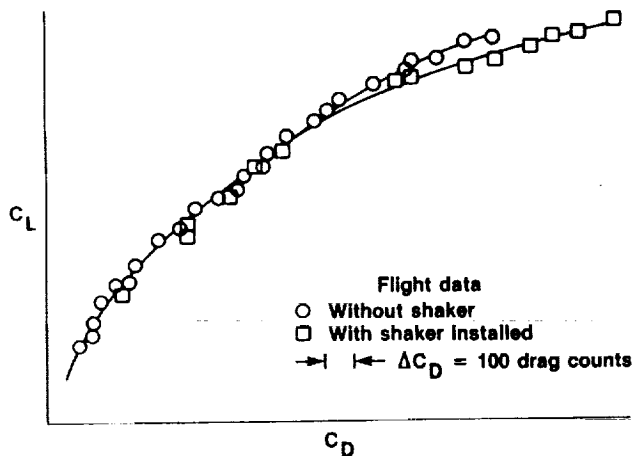
6014

Fig. 8. Effect of FCS software changes on aerodynamic performance.



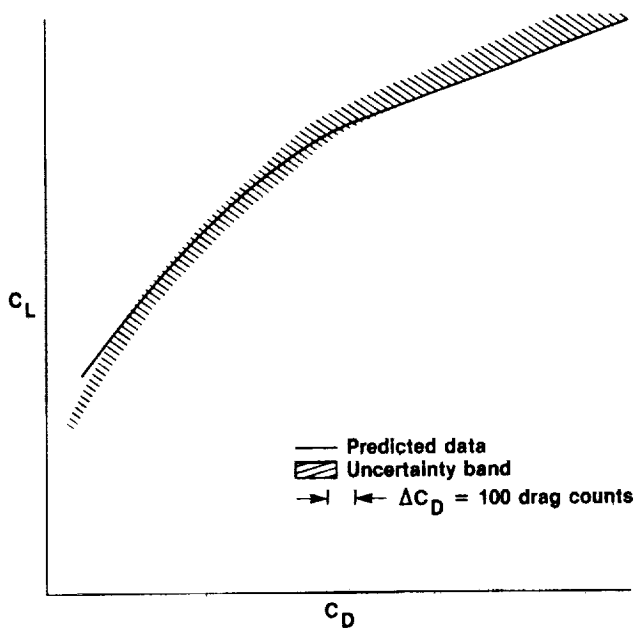
6012

Fig. 6. Flaperon shaker system fairing.



6013

Fig. 7. Effect of shaker system fairings on aerodynamic performance.



6015

Fig. 9. Effect of variations in angle-of-attack calibration on flight data.

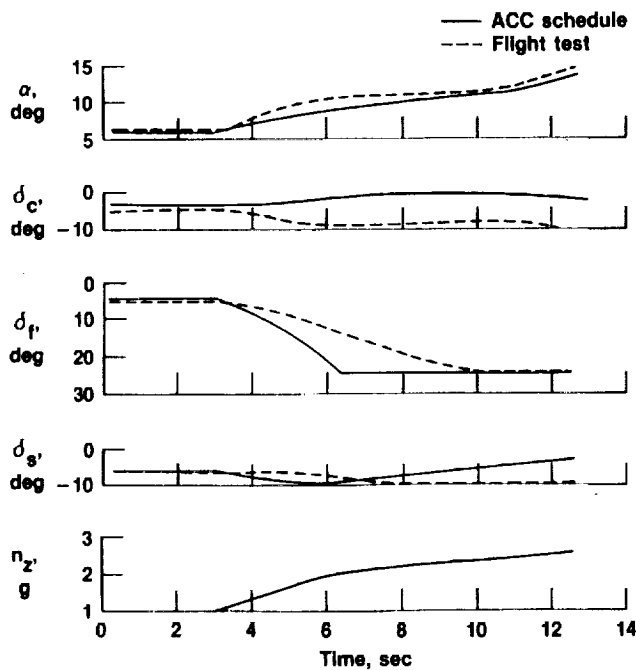


Fig. 10. Dynamic maneuver effects.

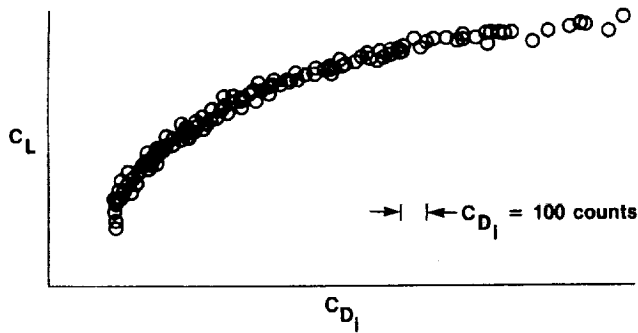
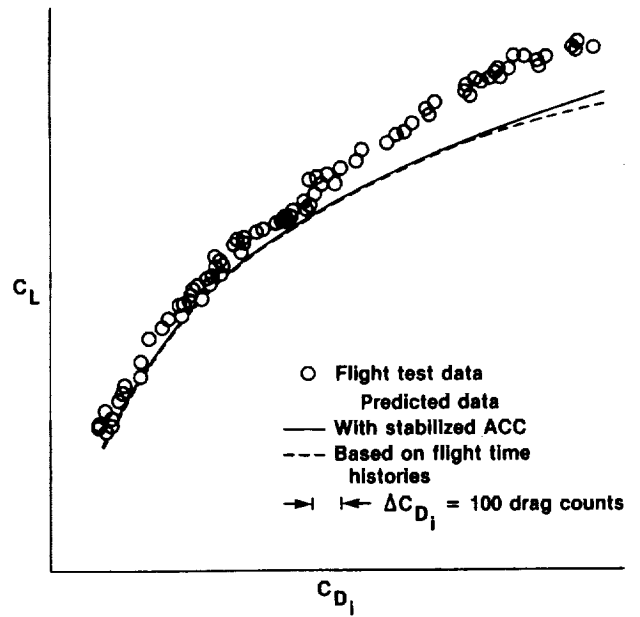
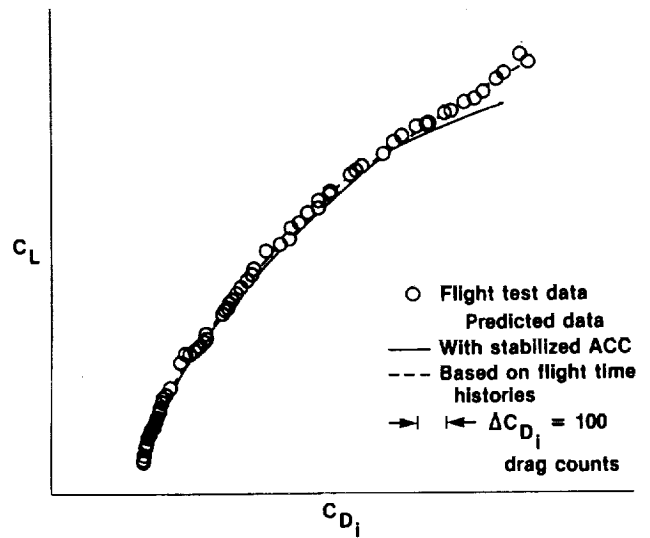


Fig. 11. Drag polar data scatter.



(a) Mach 0.8.



(b) Mach 0.9.

Fig. 12. Comparison of flight test and predicted data with induced drag.

1. Report No. NASA TM-88282		2. Government Accession No.		3. Recipient's Catalog No.	
4. Title and Subtitle  CHALLENGES IN MODELING THE X-29 FLIGHT TEST PERFORMANCE				5. Report Date January 1987	
				6. Performing Organization Code	
7. Author(s) John W. Hicks, NASA Ames-Dryden Flight Research Facility; Jan Kania, Air Force Flight Test Center, EAFB; and Robert Pearce and Glen Mills, Grumman Aerospace Corp.				8. Performing Organization Report No. H-1395	
9. Performing Organization Name and Address NASA Ames Research Center Dryden Flight Research Facility P.O. Box 273 Edwards, CA 93523-5000				10. Work Unit No. RTOP 533-02-51	
				11. Contract or Grant No.	
12. Sponsoring Agency Name and Address  National Aeronautics and Space Administration Washington, DC 20546				13. Type of Report and Period Covered Technical Memorandum	
				14. Sponsoring Agency Code	
15. Supplementary Notes  Prepared as AIAA Paper 87-0081 for presentation at AIAA 25th Aerospace Sciences Meeting, Reno, Nevada, January 12-15, 1987.					
16. Abstract  The paper presents the methods, instrumentation, and difficulties associated with drag measurement of the X-29A aircraft. The initial performance objective of the X-29A program emphasized drag polar shapes rather than absolute drag levels. Priorities during the flight envelope expansion restricted the evaluation of aircraft performance. Changes in aircraft configuration, uncertainties in angle-of-attack calibration, and limitations in instrumentation complicated the analysis. Limited engine instrumentation with uncertainties in overall in-flight thrust accuracy made it difficult to obtain reliable values of coefficient of parasite drag. The aircraft was incapable of tracking the automatic camber control trim schedule for optimum wing flaperon deflection during typical dynamic performance maneuvers; this has also complicated the drag polar shape modeling. The X-29A was far enough off the schedule that the developed trim drag correction procedure has proven inadequate. Despite these obstacles, good drag polar shapes have been developed throughout the flight envelope. Preliminary flight results have compared well with wind tunnel predictions. A more comprehensive analysis must be done to complete the performance models. The detailed flight performance program with a calibrated engine will benefit from the experience gained during this preliminary performance phase.					
17. Key Words (Suggested by Author(s))  Aircraft performance Drag polar modeling Dynamic flight test technique Forward swept wing Lift and drag				18. Distribution Statement  Unclassified - Unlimited   STAR category 05	
19. Security Classif. (of this report) Unclassified		20. Security Classif. (of this page) Unclassified		21. No. of Pages 12	
				22. Price* A02	

\*For sale by the National Technical Information Service, Springfield, Virginia 22161.